

## The growth and nonlinear evolution of helical perturbations in a swirling jet model

J. E. MARTIN <sup>a</sup>, E. MEIBURG <sup>b\*</sup>

ABSTRACT. – The growth and nonlinear evolution of a helical perturbation is investigated in a simplified swirling jet model, consisting of a line vortex along the axis surrounded by a jet shear layer with both azimuthal and streamwise vorticity. Inviscid Lagrangian vortex dynamics simulations demonstrate the mechanisms of vorticity concentration, reorientation, and stretching, as well as the nonlinear interaction and competition between a centrifugal Rayleigh instability and a Kelvin-Helmholtz instability feeding on both components of the base flow vorticity. The nonlinear evolution resulting from the interaction of these two instabilities allows for very different flow behaviors to emerge, depending on whether the helical perturbation wave and the vortex lines of the jet shear layer wind around the jet axis in the same or in opposite directions. Large-scale vortex helices evolve that can contain azimuthal vorticity either of the same or of opposite sign to that initially present in the jet shear layer. These different evolutions are triggered by the differences in the direction of the strain field set up by the evolving large-scale helix. In both cases, the generation of both signs of azimuthal vorticity due to the centrifugal Rayleigh instability allows for the possibility of unlimited growth of the helix circulation, in the absence of viscous diffusion. © Elsevier, Paris

### 1. Introduction

The present investigation continues our research into the nonlinear dynamical evolution of the vorticity field of a relatively simple model of a swirling jet. This particular model, first described by Martin and Meiburg (1994a), allows for both analytical and computational investigations of fundamental yet complex generic dynamical processes involving both shear driven and centrifugal instabilities, as well as their interactions. Here we will pay particular attention to the nonlinear growth of helically symmetric perturbations.

Swirling jets are of great practical importance, for example, in mixing and combustion problems. In such applications, they are often seen to enhance the mixing and to stabilize flames. An introduction into the basic physics of swirling flows is given by Gupta *et al.* (1984). Early analytical investigations were mostly directed at finding similarity solutions to simplified equations and boundary conditions (e.g., Wagnanski, 1970), and at determining the linear stability of various combinations of axial velocity profiles and swirl, e.g., Burggraf and Foster (1977), Stewartson (1982), Leibovich and Stewartson (1983), Toplosky and Akylas (1988), and Foster (1993). Experimental investigations of swirling jets for the most part have addressed the issue of mean flow profiles and averaged turbulent transport properties, e.g., Chigier and Chervinsky (1967), Farokhi *et al.* (1989), Frey and Gessner (1991), Mehta *et al.* (1991). Only recently have researchers begun to pay attention to the dominant role played by the underlying vortical flow structures and their dynamical evolution; e.g.

<sup>a</sup> Department of Mathematics, Christopher Newport University, Newport News, VA 23606-2998.

<sup>b</sup> Department of Aerospace Engineering, University of Southern California, Los Angeles, CA 90089-1191, USA. Phone: 213-740-5376, Fax: 213-740-7774, e-mail: eckart@spock.usc.edu

PACS: 47.15.Ki, 47.20.Cq, 47.27.Wg, 47.32.Cc.

\* Correspondence and reprints

Panda and McLaughlin (1994). These authors point out the crucial role played by axisymmetric and helical instability waves, emphasizing the importance of a *structure-based* understanding of the flow dynamics. The recent axisymmetric computational results obtained by Lopez (1990), Brown and Lopez (1990), and Lopez and Perry (1992) for an internal swirling flow, and by Krause and colleagues for the vortex breakdown phenomenon (reviewed by Althaus *et al.*, 1993), and the three-dimensional vortex dynamics simulations by the present authors for simple models of swirling flows (Martin and Meiburg, 1996) suggest that computations can provide fundamental insight into the flow physics of swirling jets.

For the purpose of studying the nonlinear dynamical interaction of shear and centrifugal instabilities in swirling jets, we recently introduced a simplified model (Martin and Meiburg, 1994a), that is an extension to earlier models proposed by Batchelor and Gill (1962), Rotunno (1978), and Caffisch, Li and Shelley (1993). The model consists of an axial centerline vortex, which is surrounded by a nominally axisymmetric vortex sheet containing both streamwise and circumferential vorticity. While this model has obvious limitations when it comes to reproducing the detailed features of experimentally generated, and often geometry dependent velocity profiles, its simplicity offers several advantages. First of all, it allows for some analytical progress (Martin and Meiburg, 1994a) in terms of a straightforward linear stability analysis, which illuminates the competition of centrifugal and Kelvin-Helmholtz instability waves. In particular, the results show that centrifugally stable flows can become destabilized by sufficiently short Kelvin-Helmholtz waves. Secondly, the model enables us to study the nonlinear interaction and competition of the various instability mechanisms involved, by means of fully nonlinear Lagrangian vortex dynamics calculations.

Some preliminary nonlinear simulations for axisymmetric perturbations were reported by Martin and Meiburg (1994b), who showed that, under certain circumstances, *counterrotating* vortex rings emerge in the braid regions between the primary vortex rings generated by the Kelvin-Helmholtz instability of the axisymmetric shear layer. These counterrotating vortex rings can trigger a dramatic decrease in the local jet diameter. A further interesting observation shows the circulation of the swirling vortex rings to be time-dependent, in contrast to the vortex rings found in nonswirling jets. Martin and Meiburg (1996) extended these earlier investigations to the three-dimensional evolution of axisymmetric waves under azimuthal perturbations. They observe that the evolution of the flow depends strongly on the initial ratio of the axisymmetric and azimuthal perturbation amplitudes. The long term dynamics of the jet can be dominated by counterrotating vortex rings connected by braid vortices, by like-signed rings and streamwise braid vortices, or by wavy streamwise vortices alone.

After a brief review of the flow model in section 2, we will investigate the nonlinear helically symmetric evolution of the above swirling jet model in more detail in section 3. Helical perturbation waves with both positive and negative azimuthal wavenumbers, will be considered. Both vorticity contours and vortex line configurations will be analyzed, along with projections of streamlines, in order to obtain a more complete picture of the temporally evolving flow field.

## 2. Flow model and numerical technique

The present flow model of an axial line vortex surrounded by a nominally axisymmetric cylindrical shear layer containing streamwise and circumferential vorticity represents an extension of earlier ones investigated by several researchers, dating back to the analyses by Batchelor and Gill (1962) as well as Rotunno (1978) of the stability of an axisymmetric layer of circular or helical vortex lines. More recently, Caffisch, Li and Shelley (1993) introduced the effect of swirl by placing the additional line vortex at the center of the axisymmetric layer. However, their unperturbed vortex sheet had an axial vorticity component only, so that a jet-like velocity component was absent. In the present investigation, we employ a slightly more complicated model (Fig. 1),

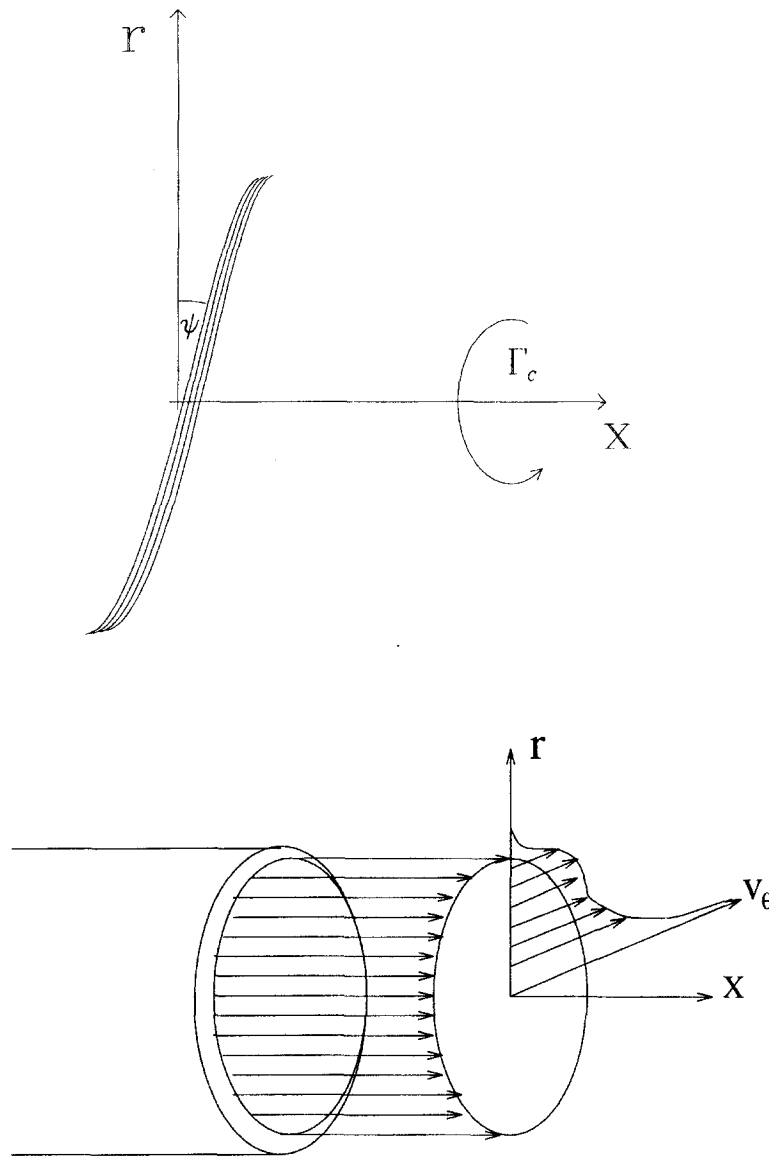


Fig. 1. – Simplified model of a swirling jet flow. The centerline vortex of strength  $\Gamma_c$  is surrounded by a nominally axisymmetric jet shear layer containing helical vortex lines of pitch  $\psi$ . The azimuthal vorticity component is related to the top hat axial velocity profile, whereas the streamwise vorticity component results in the centrifugally unstable stratification. Also shown are the streamwise and azimuthal base flow velocity profiles.

consisting of a line vortex of strength  $\Gamma_c$  at radius  $r = 0$ , surrounded by a cylindrical vortex sheet at  $r = R$ . The unperturbed axisymmetric vortex sheet contains both azimuthal vorticity (corresponding to a jump  $\Delta U_x$  in the axial velocity) and streamwise vorticity (representing a jump  $\Delta U_\theta$  in the circumferential velocity). The strength of the vortex sheet is taken to be equal and opposite to that of the line vortex. The vortex lines in the sheet hence are of helical shape, with their pitch angle  $\psi$  being

$$(1) \quad \psi = \tan^{-1} \left( \frac{\Delta U_\theta}{\Delta U_x} \right)$$

These particular features of our model were chosen on the basis of the following considerations. While an axisymmetric cylindrical layer of *circular* vortex lines represents a unidirectional flow with a top hat like profile shape, *helical* vortex lines result in an additional azimuthal velocity component, which jumps at the location of the vortex layer. If there is no streamwise circulation present at radii smaller than that of the cylindrical layer, this azimuthal velocity component vanishes inside the cylinder and exhibits a  $1/r$ -dependence on the outside. Consequently, since the magnitude of the circulation increases across the vortical layer, this flow is centrifugally stable on the basis of Rayleigh's circulation theorem. However, if some streamwise circulation is contained inside the cylinder, and if this circulation is of opposite sign to the streamwise circulation of the layer itself, then the magnitude of the circulation can decrease across the vortical layer, so that we obtain a centrifugally unstable flow. The line vortex at the center of the jet is introduced exactly for this purpose. Its strength is taken to be equal and opposite to that of the streamwise circulation contained in the vortical layer, in order that the azimuthal velocity component of the base flow vanishes outside the jet. In this way, our simplified model mimics a swirling jet entering fluid at rest. The fluid velocity profile associated with our model is sketched in Figure 1 as well.

By introducing both axial and azimuthal vorticity along with the central line vortex, this model allows for the investigation of competing Kelvin-Helmholtz and centrifugal instabilities, which can be expected to lead to interesting nonlinear dynamical behavior. For the nonswirling top hat jet velocity profile it is known that axisymmetric and helical perturbations will result in the formation of vortex rings or helices, respectively, all of the same sign (Martin and Meiburg, 1991, 1992). For purely swirling flow, on the other hand, Caffisch *et al.* (1993) demonstrated that axisymmetric perturbations lead to the emergence of counterrotating vortex rings. By superimposing a top hat streamwise velocity profile upon the purely swirling flow, a breaking of the symmetry exhibited by the purely swirling flow alone occurs. In the present investigation, our goal is to simulate the nonlinear growth of a helical perturbation, characterized by a given streamwise wavelength and an azimuthal wavenumber  $m$ .

In order to compute the nonlinear evolution of the flow in response to certain imposed perturbations, we employ a vortex filament technique that is essentially identical to the one used in earlier investigations of plane shear layers, wakes, and jets (Ashurst and Meiburg, 1998; Meiburg and Lasheras, 1988; Masheras and Meiburg, 1990; Martin and Meiburg, 1991, 1992, 1994b, 1996). It is based on the theorems of Kelvin and Helmholtz and follows the general concepts reviewed by Leonard (1985) and Meiburg (1995). A detailed account of the technique is provided in these earlier references. For the numerical simulations of the simple jet model, we limit ourselves to the temporally growing problem.

One streamwise wavelength is typically discretized into 205 filaments. Each filament initially contains 35 segments per streamwise wavelength of the perturbation wave. This number increases as the filaments undergo significant deformation, which requires a remeshing procedure that leads to a successively finer discretization, up to approximately 40,000 nodes at the end of the simulation. The above numerical parameters emerged from test calculations, in which we refined the discretization until a further increase in resolution resulted in very small changes. The Biot-Savart integration is carried out with second order accuracy both in space and in time by employing the predictor-corrector time-stepping scheme, in conjunction with the trapezoidal rule for the spatial integration. The time-step is repeatedly reduced as local acceleration effects increase. The filament core radius  $\sigma$  decreases as its arclength increases, to conserve its total volume.

We take the streamwise velocity difference between the centerline and infinity as the characteristic velocity. The axisymmetric shear layer thickness serves as the characteristic length scale, which results in the filament core radius  $\sigma = 0.5$ . The nominal jet radius  $R$  is taken to be 5, and we obtain the ratio of jet radius  $R$  and momentum thickness  $\theta$  of the jet shear layer as  $R/\theta = 22.6$ . Hence, the ratio  $R/\sigma \gg 1$ , and we are well within the range of validity of the filament model.

### 3. Results

#### 3.1. $m = -2$

We begin by discussing the evolution of a helical wave with a streamwise wavelength of approximately  $2\pi$ , and an azimuthal wavenumber of  $m = -2$ . In this case, the helical perturbation wave winds around the jet centerline in the same direction as the helical vortex lines. The initial helical perturbation displaces the vortex filament centerlines in the radial direction, with an amplitude of five per cent of the nominal jet radius. A typical development of the flow field is shown in Figure 2 for the relatively large velocity ratio of  $\Delta U_\theta / \Delta U_x = 8.2$ . This value indicates that the jump in the azimuthal velocity component across the jet shear layer is much larger than that of the axial component, so that, for the unperturbed flow, the vortex lines are predominantly oriented in the streamwise direction. Figure 2 shows a number of side views, i.e., those filament sections located at  $y > 0$ , of the configuration of vortex filaments, for the times 0.039, 0.430, 0.625, 0.820 and 0.947. For clarity, two streamwise wavelengths are shown. The roll-up of the vorticity layer into a large-scale helical vortex structure is clearly visible. Here it is important to notice that the azimuthal vorticity of the large-scale helix is of the same sign as the azimuthal vorticity initially present in the jet shear layer. Already very early on, this evolving vortex helix generates a strain field that changes the direction of the vortex lines residing in the braid region. In particular, the sign of the azimuthal vorticity component in the braid region is reversed, so that the azimuthal braid vorticity points in the opposite direction to the azimuthal vorticity making up the large scale helix. This behavior is clearly reflected in the azimuthal vorticity contours of a longitudinal cut through the flow, shown in Figure 3 for the same times as above. These cuts demonstrate the concentration of vorticity into helical vortex cores, along with the formation of elongated braids connecting the cores. The reversal of the sign of the braid vorticity is apparent, leading to a situation in which cores and braids contain azimuthal vorticity of opposite signs.

Our earlier investigation of the evolution of axisymmetric perturbations in a swirling jet (Martin and Meiburg, 1996) showed a similar behavior there, which eventually led to the emergence of concentrated braid vortex rings, of a sign opposite to that of the primary rings. While the present simulation has not been carried far enough in time to display the emergence of a concentrated counterrotating helical structure, this appearance of azimuthal braid vorticity of the opposite sign nevertheless reflects the influence of the centrifugal Rayleigh instability and its tendency to generate pairs of counterrotating vortical structures. Similarly to the axisymmetric case, the swirl generates a strong radial gradient of the azimuthal velocity component. As a result, this velocity component of a vortex line varies strongly along its arclength. Thus, there are segments of a vortex line that travel around the jet's axis at a higher angular velocity than neighboring segments of the same vortex line. Since the overall dynamics is inviscid, the vortex line has to stay connected, so that it necessarily has to fold back and forth, thereby generating azimuthal vorticity components of both signs.

The emergence of opposite-signed braid vorticity is further reflected by Figure 4, which shows the directional velocity field in a plane of constant azimuthal angle. The sense of fluid rotation in the braid region is clearly opposite to that in the large scale helix.

In this context, it is interesting to note that, at a fixed azimuthal position, the integral over one streamwise wavelength of the azimuthal vorticity has to stay constant with time, equal to the value determined by the initial axial and azimuthal velocity jumps, and by the perturbation wavelength. However, within that streamwise wavelength, the circulation of the helix core and the braid can vary, as long as they add up to this constant overall circulation. In particular, with time the helix core and the braid can develop stronger and stronger circulations of opposite sign, in a fashion similar to the counterrotating vortex rings of our earlier analyses. Thus, in the absence of viscous diffusion, there are no mechanisms that can limit the growth of the circulation of the helix.

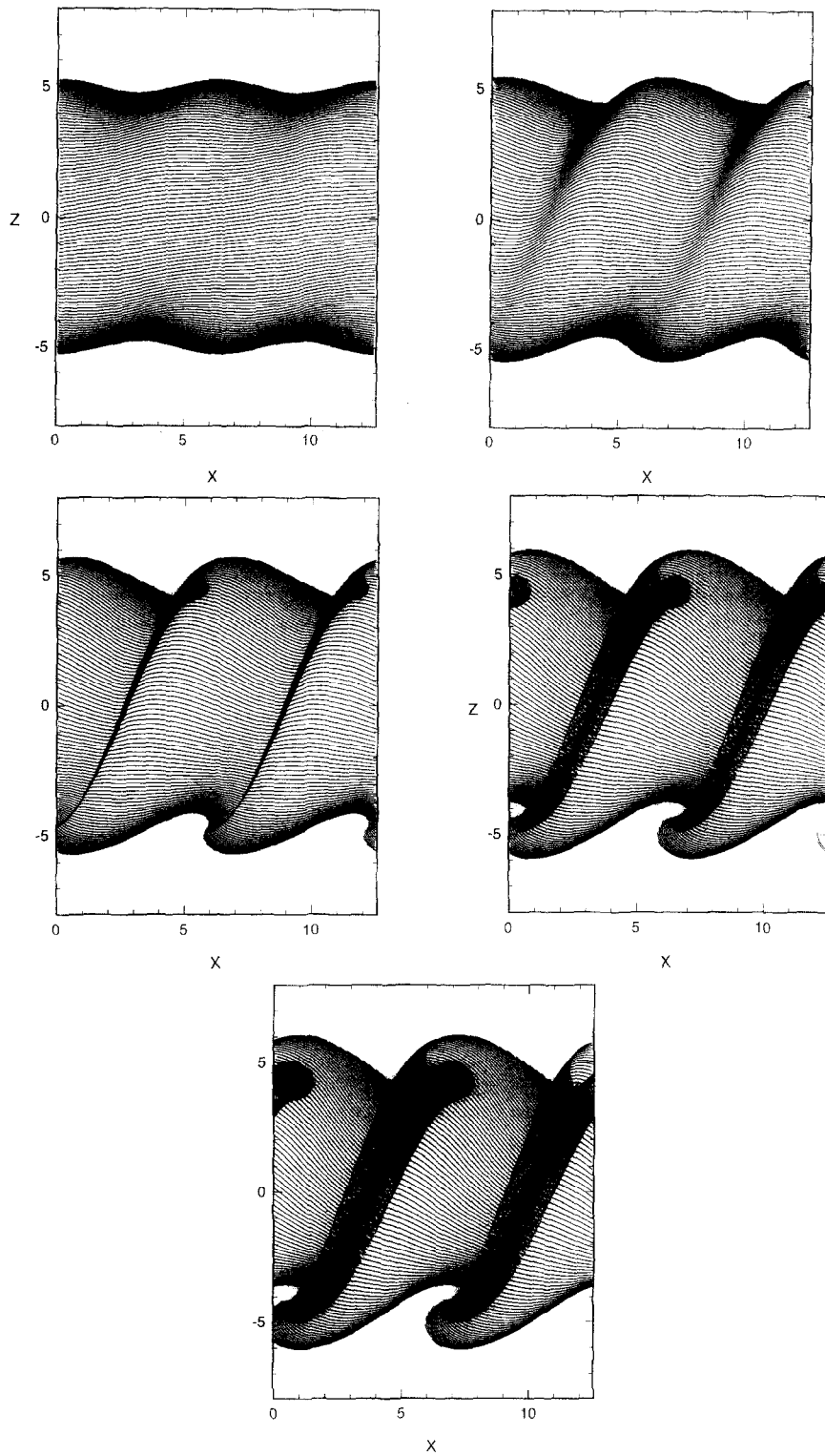


Fig. 2. – The evolution of a swirling jet with  $\Delta U_\theta/\Delta U_r = 8.2$  subject to a helical perturbation with  $m = -2$ . Shown are side views of the vortex filaments at times 0.039, 0.430, 0.625, 0.820, and 0.947. For clarity, two streamwise wavelengths are shown. Note the roll-up of the jet shear layer into a large-scale vortex helix, as well as the reorientation of the braid vortex line segments into the opposite azimuthal direction.

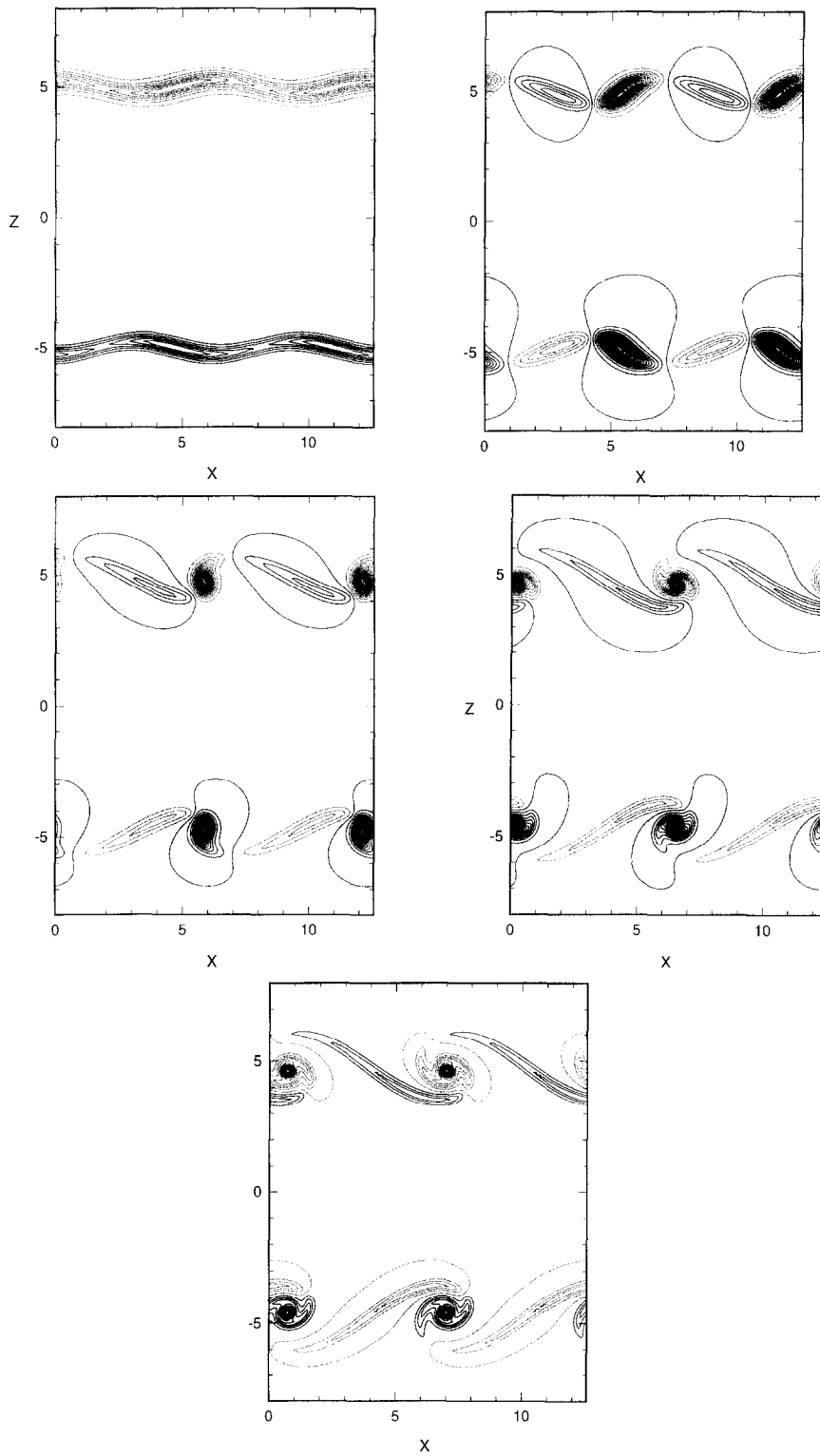


Fig. 3. -  $m = -2$ : Contours of the azimuthal vorticity component at the same times as in Figure 2. These contour plots as well indicate the roll-up into a large-scale vortex helix, along with the emergence of opposite-signed azimuthal braid vorticity, a manifestation of a centrifugal Rayleigh instability.

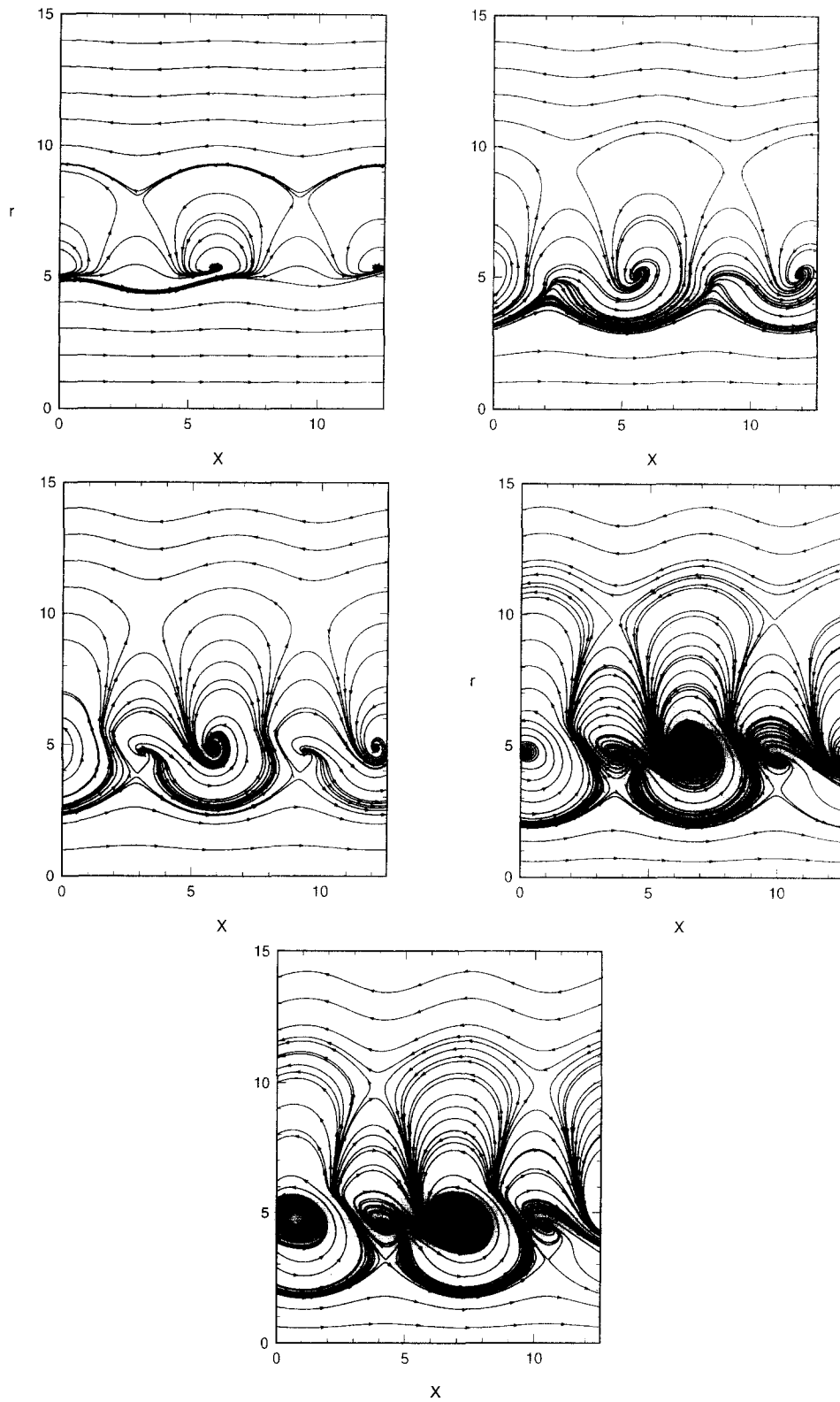


Fig. 4.  $-m = -2$ : The directional velocity field in a plane of constant azimuthal angle, for the same times as in Figure 2. The counterrotating fluid motion in the helix core and the braid is clearly visible.



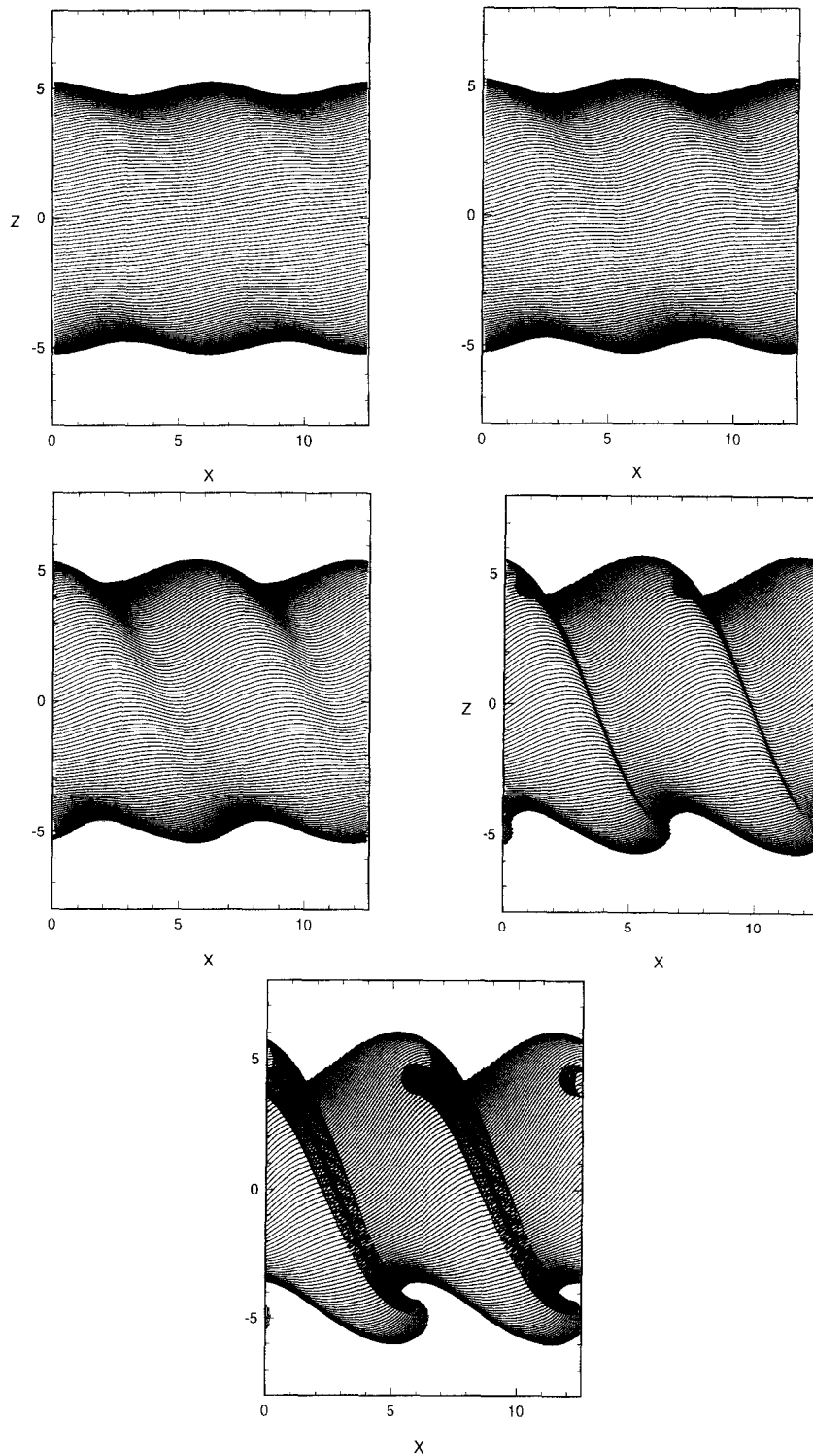


Fig. 5. – The evolution of a swirling jet with  $\Delta U_\theta/\Delta U_x = 8.2$  subject to a helical perturbation with  $m = 2$ . Shown are side views of the vortex filaments at times 0.039, 0.234, 0.430, 0.684, and 0.908. The helical perturbation wave and the vortex lines of the jet shear layer wind around the jet axis in opposite directions. In contrast to the  $m = -2$  case, the vortex lines now reverse their azimuthal direction in the core region, rather than in the braid region.

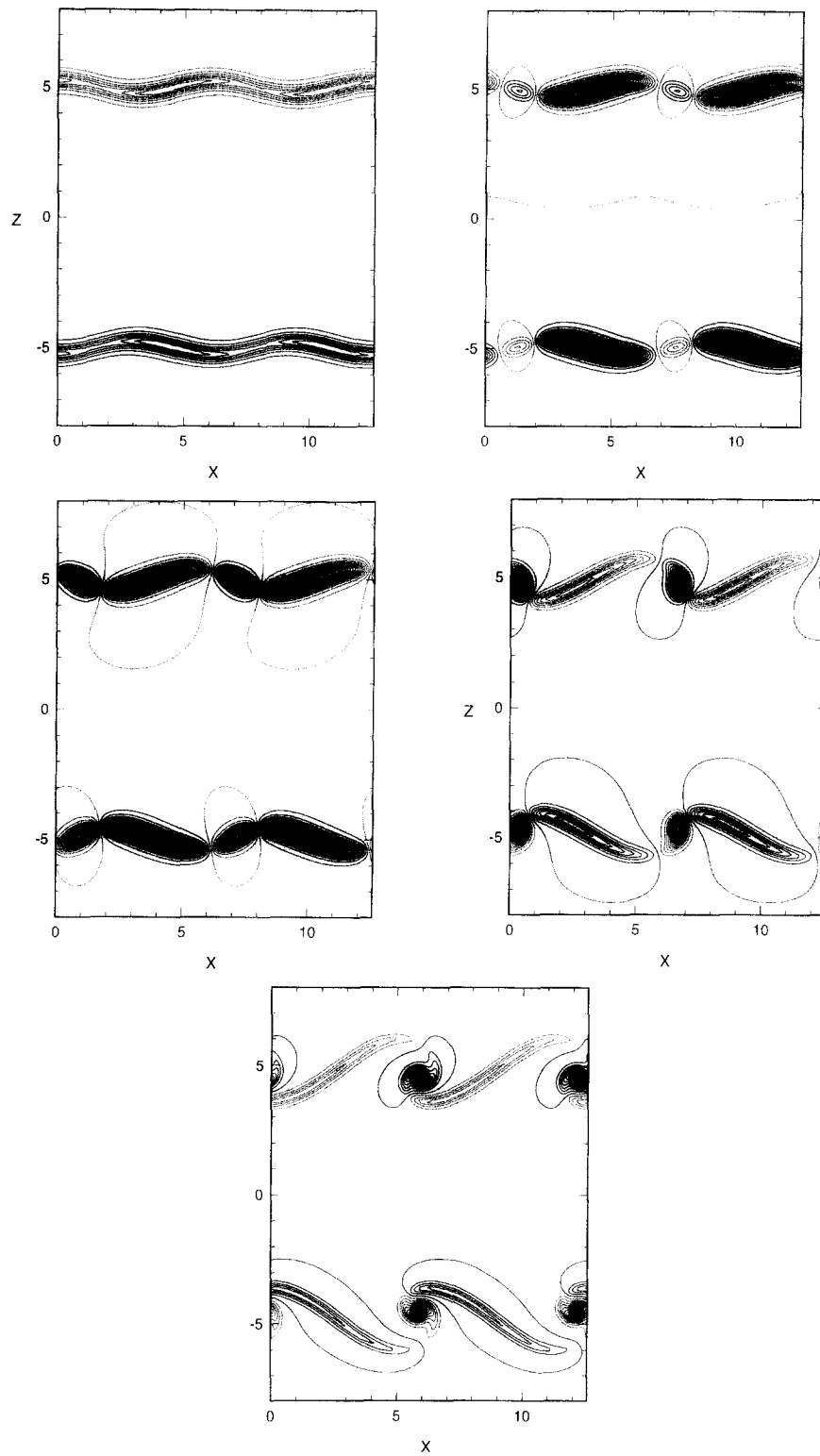


Fig. 6.  $-m = 2$ : Contours of the azimuthal vorticity component at the same times as in Figure 5. Note that the jet flows from left to right, i.e., in the  $+x$ -direction.

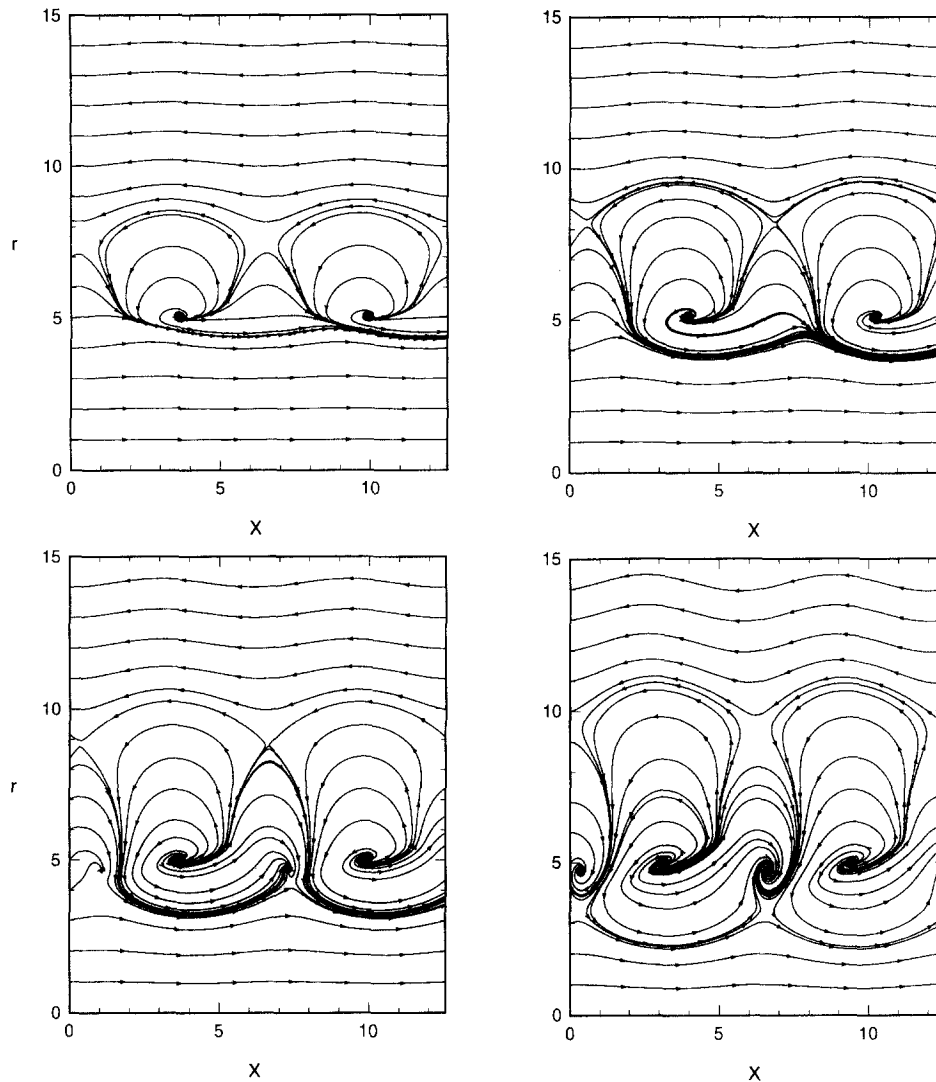


Fig. 7. –  $m = 2$ : The directional velocity field in a plane of constant azimuthal angle, at times 0.039, 0.234, 0.430, and 0.684.

### 3.2. $m = 2$

It is interesting to contrast the above evolution of the swirling jet model with that obtained for  $m = 2$ , i.e., a helical perturbation of opposite azimuthal wavenumber. Now the helical perturbation winds around the jet axis in the direction opposite to that of the jet shear layer vortex lines, which has a profound effect on the ensuing nonlinear evolution. Side views of the vortex filament configurations at times 0.039, 0.234, 0.430, 0.684, and 0.908 are shown in Figure 5. Again, the emerging large-scale helical structure affects the orientation of the vortex lines, but in a very different way compared to the  $m = -2$  case described above. The strain field generated by the evolving helix now *amplifies* the azimuthal braid vorticity from the start, rather than reversing it, as for  $m = -2$ . At the same time, the sign of the azimuthal vorticity component in the emerging core region of the vortex helix changes, as the vortex lines making up the large-scale helix reverse their azimuthal direction. As a result, the vortex helix is made up of azimuthal vorticity of the opposite sign to that initially present in the jet shear layer, while the sign of the braid vorticity remains unchanged. This behavior is in contrast to the case

$m = -2$  described above. The difference is caused by the change in the strain field, whose extensional axis is approximately binormal to the core of the helix. Depending on the alignment of this extensional direction with the direction of the braid vortex lines, the azimuthal component of the latter is either amplified or reversed.

The crosscuts shown in Figure 6 for the identical times further demonstrate this behavior. Having in mind typical flow visualizations of nonswirling jets, one is tempted, at first glance, to associate the cross-cuts depicted in Figure 6 with a jet flowing from right to left, i.e., in the  $-x$ -direction. This is due to the fact that the azimuthal jet shear layer vorticity, once it concentrates into large-scale structures, typically shrinks the jet diameter upstream of the large-scale structures, while widening it downstream. However, in the present swirling flow, the large-scale structures are made up azimuthal vorticity which is opposite in sign to that of the initial jet shear layer, so that it increases the jet diameter upstream of the helix core and reduces it on the downstream side. The directional velocity field in a plane of constant azimuthal angle shown in Figure 7 for times 0.039, 0.234, 0.430, and 0.684(?) confirm that the jet indeed flows into the  $+x$ -direction. The reason for this lies in the larger absolute magnitude of the braid circulation, as compared to the core circulation.

#### 4. Summary and Conclusions

The present investigation represents an attempt to study the main mechanisms resulting in the complex nonlinear dynamical evolution of swirling jets subject to helical perturbations, by performing Lagrangian vortex dynamics simulations for a simplified model that nevertheless contains the essential features characterizing such flows. The model consists of a line vortex, surrounded by an axisymmetric vortex sheet containing both azimuthal and streamwise vorticity. The axial, jet-like velocity profile gives rise to a Kelvin-Helmholtz instability, thereby leading to the formation of a large-scale vortex helix. The additional azimuthal velocity component of the base flow introduces streamwise vorticity as well, whose existence allows for a centrifugal instability to develop.

In general, the addition of swirl is found to lead to significantly more complex nonlinear dynamical behavior of the flow. We observe that the nonlinear evolution resulting from the interaction of these two instabilities allows for very different flow behaviors to emerge, depending on whether the helical perturbation wave and the jet shear layer vortex lines wind around the jet axis in the same or in opposite directions. In the former situation (our case  $m = 2$ ), a large-scale vortex helix evolves which contains azimuthal vorticity of the same sign as that initially present in the jet shear layer. The strain field generated by this vortex helix reorients the braid vortex lines, thereby reversing their azimuthal component. In the absence of viscous diffusion, this mechanism allows the helix circulation to grow without bounds.

If the helical perturbation wave winds around the jet axis in the opposite direction to the jet shear layer vortex lines (our case  $m = 2$ ), a qualitatively very different behavior ensues. Now the azimuthal vorticity component reverses its direction in the core region of the emerging large-scale vortex helix, while it remains unchanged in the braids connecting successive core regions. The dominant vortical flow structure thus consists of azimuthal vorticity of opposite sign to that initially present in the jet shear layer. In summary, the relative orientations of the extensional strain field generated by the large-scale helical structure and the vortex lines of the jet shear layer determine the nature of the emerging dominant flow structures, and as a result the global evolution of the flow.

The above description represents only a first step, and a more detailed investigation is clearly necessary. In particular, it will be of interest to study the evolution of the flows described above under the influence of additional, azimuthal perturbations. Furthermore, the interaction of helical perturbation waves of opposite signs needs to be addressed.

**Acknowledgements.** – Support by the National Science Foundation to EM is gratefully acknowledged. JEM was supported by the National Aeronautics and Space Administration under NASA Contract No. NAS1-19480 while in residence at the Institute for Computer Applications in Science and Engineering (ICASE), NASA Langley Research Center. Computing resources were provided by the NSF-supported San Diego Supercomputer Center.

## REFERENCES

- ALTHAUS W., BRUCKER C., WEIMER M., 1995, Breakdown of slender vortices, in: *Fluid Vortices*, ed. S.I. Green, Kluwer.
- ASHURST W.T., MEIBURG E., 1988, Three-dimensional shear layers via vortex dynamics, *J. Fluid Mech.*, **189**, 87.
- BATCHELOR G.K., GILL A.E., 1962, Analysis of the stability of axisymmetric jets, *J. Fluid Mech.*, **14**, 529.
- BROWN G.L., LOPEZ J.M., 1990, Axisymmetric vortex breakdown. Part 2: Physical mechanism, *J. Fluid Mech.*, **221**, 553.
- BURGGRAF O.R., FOSTER M.R., 1977, Continuation or breakdown in tornado-like vortices, *J. Fluid Mech.*, **80**, 645.
- CAFLISCH R.E., LI X., SHELLEY M.J., 1993, The collapse of an axisymmetric swirling vortex sheet, *Nonlinearity*, **6**, 843.
- CHIGIER N.A., CHERVINSKY A., 1967, Experimental investigation of swirling vortex motion in jets, *Trans. ASME, J. Appl. Mech.*, **34**, 443.
- FAROKHI S., TAGHAVI R., RICE E.J., 1989, Effect of initial swirl distribution on the evolution of a turbulent jet, *AIAA J.*, **27**, 700.
- FOSTER M.R., 1993, Nonaxisymmetric instability in slowly swirling jet flows, *Phys. Fluids A*, **5**, 3122.
- FREY M.O., GESSNER F.B., 1991, Experimental investigation of coannular jet flow with swirl along a centerbody, *AIAA J.*, **29**, 2132.
- GASTER M., 1962, A note on the relation between temporally-increasing and spatially-increasing disturbances in hydrodynamic stability, *J. Fluid Mech.*, **14**, 222.
- GUPTA A.K., LILLEY D.G., SYRED N., 1984, *Swirl Flows*, Kent, Engl: Abacus.
- LASHERAS J.C., MEIBURG E., 1990, Three-dimensional vorticity modes in the wake of a flat plate, *Phys. Fluids A*, **2**, 371.
- LEBOVICH S., STEWARTSON K., 1983, A sufficient condition for the instability of columnar vortices, *J. Fluid Mech.*, **126**, 335.
- LEONARD A., 1985, Computing three-dimensional flows with vortex elements, *Ann. Rev. Fluid Mechanics*, **17**, 523.
- LOPEZ J.M., 1990, Axisymmetric vortex breakdown. Part 1: Confined swirling flow, *J. Fluid Mech.*, **221**, 533.
- LOPEZ J.M., PERRY A.D., 1991, Axisymmetric vortex breakdown. Part 3: Onset of periodic flow and chaotic advection, *J. Fluid Mech.*, **234**, 449.
- MARTIN J.E., MEIBURG E., 1991, Numerical investigation of three-dimensionally evolving jets subject to axisymmetric and azimuthal perturbations, *J. Fluid Mech.*, **230**, 271.
- MARTIN J.E., MEIBURG E., 1992, Numerical investigation of three-dimensionally evolving jets under helical perturbations, *J. Fluid Mech.*, **243**, 457.
- MARTIN J.E., MEIBURG E., 1994a, On the stability of the swirling jet shear layer, *Phys. Fluids*, **6**, 424.
- MARTIN J.E., MEIBURG E., 1994b, The nonlinear evolution of swirling jets, *Meccanica*, **29**, 331.
- MARTIN J.E., MEIBURG E., 1996, Nonlinear axisymmetric and three-dimensional vorticity dynamics in a swirling jet model, *Phys. Fluids*, **8**, 1917.
- MEHTA R.D., WOOD D.H., CLAUSEN P.D., 1991, Some effects of swirl on turbulent mixing layer development, *Phys. Fluids A*, **3**, 2716.
- MEIBURG E., 1995, Three-dimensional vortex dynamics simulations, in: *Fluid Vortices*, ed. S.I. Green, Kluwer.
- MEIBURG E., LASHERAS J.C., 1988, Experimental and numerical investigation of the three-dimensional transition in plane wakes, *J. Fluid Mech.*, **190**, 1.
- MICHALKE A., HERMANN G., 1982, On the inviscid instability of a circular jet with external flow, *J. Fluid Mech.*, **114**, 343.
- PANDA J., McLAUGHLIN D.K., 1994, Experiments on the instabilities of a swirling jet, *Phys. Fluids*, **6**, 263.
- ROTUNNO R., 1978, A note on the stability of a cylindrical vortex sheet, *J. Fluid Mech.*, **87**, 761.
- STEWARTSON K., 1982, The stability of swirling flows at large wavenumber when subjected to disturbances with large azimuthal wavenumber, *Phys. Fluids*, **25**, 1953.
- TOPLOSKY N., AKYLAS T.R., 1988, Nonlinear spiral waves in rotating pipe flow, *J. Fluid Mech.*, **190**, 39.
- WYGNANSKI I., 1970, Swirling axisymmetrical laminar jet, *Phys. Fluids*, **13**, 2455.

(Received 25 June 1997,  
revised and accepted 08 December 1997)